

# Climatology of the Sierra Nevada Mountain Wave Events

Vanda Grubišić\* and Brian J. Billings

Desert Research Institute

Reno, Nevada

*Revised manuscript submitted to the*

*Monthly Weather Review*

April 5, 2007

\* *Corresponding author address:* Vanda Grubišić, Division of Atmospheric Sciences, Desert Research Institute, 2215 Raggio Parkway, Reno, NV 89512. E-mail: Vanda.Grubic@dri.edu

## **Abstract**

This note presents a satellite-based climatology of the Sierra Nevada mountain wave events. The data presented was obtained by detailed visual inspection of visible satellite imagery to detect mountain lee wave clouds based on their location, shape, and texture. Consequently, this climatology includes only mountain wave events during which sufficient moisture was present in the incoming air stream and whose amplitude was large enough to lead to cloud formation atop mountain wave crests. The climatology is based on data from two mountain wave seasons in the 1999 to 2001 period. Mountain wave events are classified in two types according to cloud type as lee wave trains and single wave clouds. The frequency of occurrence of these two wave types is examined as a function of the month of occurrence (October to May) and region of formation (north, middle, south, or the entire Sierra Nevada range).

Results indicate that the maximum number of mountain wave events in the lee of the Sierra Nevada occurs in the month of April. For several months, including January and May, frequency of wave events displays substantial interannual variability. Overall, trapped lee waves appear to be more common, in particular in the lee of the northern Sierra. A single wave cloud on the lee side of the mountain range was found to be a more common wave form in the southern Sierra Nevada. The average wavelength of the Sierra Nevada lee waves was found to lie between 10 and 15 km, with a minimum at 4 km and a maximum at 32 km.

# 1 Introduction

There are several mountain ranges worldwide that are well-known for generation of large-amplitude mountain waves such as the Alps, the Andes, or the New Zealand Alps. In the United States, the most thoroughly documented is the Colorado Front Range (e.g., Lilly and Zipser 1972; Clark et al. 2000). Another, the Sierra Nevada in California (Fig. 1) has been until recently less well-known among scientists, but equally well known among amateur and professional pilots, for its generation of large-amplitude lee waves, rotors, strong updrafts and clear-air turbulence (Holmboe and Klieforth 1957; Kuettner 1959; Whelan 2000).

The Sierra Nevada is an approximately 100 km wide and 600 km long quasi-two-dimensional mountain range that forms part of the western rim of the Great Basin. Several factors, including the gentle upwind and steep lee-side slopes, make the Sierra Nevada an excellent mountain wave generator. Due to the absence of significant topography upwind, lee side disturbances are almost exclusively generated by the main massif of the Sierra Nevada range. Additionally, the proximity of the Pacific Ocean provides a source of upper-level moisture that commonly gives rise to clouds atop the mountain wave crests.

Conducting a climatology of mountain wave events in the Sierra Nevada is difficult due to the lack of routine measurements that can be directly and unambiguously related to mountain wave activity. While mountain waves do have a profound effect on the state of the atmosphere, only occasionally are they associated with easily detectable strong lee side surface winds. VHF radar wind profilers have been successfully used to observe mountain wave activity (Ralph et al. 1992; Worthington and Thomas 1996; Vosper and Worthington 2002). The boundary-layer wind profilers (UHF) were also successfully used in capturing signatures of mountain wave activity (Brown et al. 2005) in the recent Sierra Rotors Project (SRP) and the Terrain-induced Rotor Experiment (T-REX) observational campaigns (Grubišić et al. 2004). However, while the wind

profilers are clearly useful in documenting mountain wave activity, currently there are no routine wind profiler measurements along the lee side of the Sierra Nevada.

As mountain lee waves provide one of the very few obviously and measurably periodic phenomena seen in cloud formations, studying this phenomenon is a good candidate for application of satellite imagery. Since the early days of satellite meteorology, and in particular with increasing sensor resolution of meteorological satellites, it has become evident that satellite imagery provides a wealth of information on small-scale atmospheric processes in addition to the large-scale synoptic features (Scorer 1986). Application of satellite imagery to study of orographically-induced phenomena such as mountain waves and mountain wakes has a long history (Hubert and Krueger 1962; Conover 1964; Fritz 1965; Chopra and Hubert 1965). Satellite imagery continues to be actively used in mountain wave research today (e.g., Ralph et al. 1997; Smith et al. 1997; Pan and Smith 1999), where, as is true for mesoscale meteorological studies in general, it is most effective when used in conjunction with data from other sensors such as surface weather stations, soundings, radars, or in situ measurements by research aircraft in field campaigns (Smith and Grubišić 1993; Johnson et al. 1994). However, with long uninterrupted records, satellite data is also ideal for climatological studies of mesoscale phenomena (Banta and Schaaf 1987; Moore and Renfrew 2005). In this study of mountain waves, in what effectively is a data-sparse region, we rely primarily on the utilization of high-resolution visible satellite imagery for detection of lee wave clouds based on their location, shape, and texture.

With many potential benefits to forecasters, climatologists, mesoscale and regional climate modelers, and for selecting optimal sites and timing of observational field campaigns\* existence of such climatologies is clearly important. Additionally, availability of climatologies for different

---

\*Preliminary results from this study were used as guidance for the selection of the T-REX field campaign timing and location.

mountain ranges that are known for generation of lee waves (Auer 1992; Mitchell et al. 1990; Smith 1976; Vosper and Mobbs 1996) would allow for easier generalization of physical process study findings obtained in one region to other such regions in the world.

This note is organized as follows. Section 2 describes the source of data and the method of analysis. Climatology results are presented and discussed in section 3. Section 4 concludes the note.

## 2 Data Sources and Analysis Methods

Mountain lee wave clouds in the lee of the Sierra Nevada were identified by visual inspection of visible satellite imagery from the NOAA's Geostationary Operational Environmental Satellite (GOES-10). GOES-10 visible images were available to us at 1 km horizontal resolution in fifteen minute intervals during daylight hours for the two-year period from 1999 to 2001. High temporal frequency and fixed field of view of this satellite, made the GOES-10 imagery particularly suitable for this study, which takes advantage of regular sequential observations of cloud patterns.

For mountain waves to form, vertical profiles of thermal stability and wind of the approaching air stream need to be able to support sustained oscillatory motions. Favorable conditions for wave activity include strong cross-mountain winds, and elevated inversions at or near the ridge-top height. In addition to a sufficiently large wave amplitude, for a wave pattern to become visible in satellite imagery moisture is needed through a sufficiently thick atmospheric depth. Conditions necessary for mountain wave and wave cloud formation in the lee of the Sierra Nevada are typically found near frontal zones associated with mid-latitude cold fronts (Holmboe and Klieforth 1957). During summer, dry conditions and weaker westerly flows make mountain wave clouds relatively rare along the Sierra Nevada lee. Consequently, we have focused on the months of October to May as the Sierra Nevada mountain wave season, during which mid-latitude synoptic systems travel past this

mountain range, producing conditions favorable for mountain wave formation.

We have selected the visual inspection method for detection of cloud types associated with mountain waves. While automated systems for interpretation of satellite imagery have been developed for specific applications (Peak and Tag, 1992), the pattern recognition abilities of the human eye/brain apparatus remain superior to automated procedures. The same set of satellite images was independently visually inspected by two analysts and their findings subsequently compared and merged. As the imagery interpretation expertise requires a combination of skills, including both pattern recognition and the expertise of inferring the meteorological meaning of those patterns, both analysts underwent training on an independent data set first.

The observed wave clouds were classified in two categories based on the appearance in satellite images. The two categories are: i) lee wave trains, and ii) single wave (“arch”) clouds. These two types are illustrated in Fig. 2, and correspond to the following two types in the classification of orographic cloud patterns by Conover (1964): i) the wavelike pattern due to lee waves, and ii) the isolated lenticular category. For the first type, vertical propagation of wave energy is limited, by a sharp increase of the cross-mountain wind with height or a pronounced mountain-top inversion or a combination of the two factors, resulting in a low-level wave pattern that can extend significant horizontal distances from the generating terrain (Smith 1979). Resulting wavelike pattern consists of approximately parallel cloud bands corresponding to the crests of waves induced by the flow of air over a ridge-like obstacle (Figs. 2b,d). In contrast, mountain waves giving rise to the second type of wave clouds typically occur when wind direction, speed and stability tend to be more uniform through a deep layer of atmosphere, allowing vertical wave energy propagation and generation of mid- to high-level clouds. For large obstacles, such as the Sierra Nevada, these waves are mostly hydrostatic, implying nearly vertical wave energy propagation, and, as viewed from the top, a single wave crest located in the immediate lee of the generating mountain range (Figs. 2a,c).

There are several prominent characteristics of mountain waves and wave clouds that can be used to visually identify them in satellite images. Most important is a narrow formation region on the lee side of a mountain range. Given the orographic origin, the cloud is likely to follow the orientation of the mountain range (Fig. 2d). Also, wave clouds tend to be somewhat elliptical and smoother than most clouds, in particular those in the single wave cloud category (Figs. 2a,c). This unique shape and texture allow wave clouds to be distinguished from other cloud formations, such as orographic cumulus convection, frontal bands, cumulonimbus, and in particular, cloud streets. Another distinctive feature of wave clouds is the presence of the Foehn gap, a slim area of clear skies directly to the lee of the mountain range (Fig. 2d). This clear slot is caused by the subsidence of air in the lee of the mountain. Since the mountain range of interest is snow covered for the major part of the selected October to May period, it is important to distinguish between wave clouds and snow covered surfaces. Often, mountain valleys remain snow free, which gives snow cover over the mountains a characteristic dendritic appearance. Also, snow shows at a slightly darker tone than clouds in our two categories. Deeper into the winter, questionable cases can be resolved by examining infrared imagery, since cloud top temperatures are generally colder than surface snow.

In addition to the wave cloud type, the month and general geographic region in which the clouds formed were recorded. For the latter, we have defined four regions of formation (Fig. 1). The northern region extends from the north end of the Sierra Nevada to the latitude of Topaz Lake, NV ( $38.46^\circ$  N,  $118.50^\circ$  W); the extent of the southern region is from the north end of the White-Inyo Mountains ( $37.63^\circ$  N,  $118.26^\circ$  W) to the south end of the Sierra Nevada, whereas the central region bridges the above two. A fourth category was created for wave clouds that form along the entire length of the Sierra range (Fig. 2c). Occasionally, a single wave cloud is combined with a cirrus “cloud plume” (Conover 1964; Jiang and Doyle 2006), which can extend considerable distances downwind (Fig. 2d). In case of a long wave cloud such as that shown in Fig. 2d, the cirrus

plume has an appearance of a cloud deck that can partially or completely mask lower level clouds. Finally, we have also recorded the event duration and, for the lee wave trains, the wavelength. The latter was taken to be the measured distance downwind of the obstacle with the wave pattern, divided by the number of waves in the interval.

At this point, it is appropriate to discuss some of the limitations of this particular method. The most important limitation is that, while all mountain wave clouds are caused by mountain waves, not all mountain waves will induce cloud formation. This is especially true in the case of small amplitude waves and insufficient moisture. Since this method utilizes the identification of wave clouds, “dry mountain waves” will be absent from this climatology. The exclusion of the dry summer months is beneficial in this respect, but this problem can still occur throughout the year.

The number of wave clouds can also be underestimated due to three additional factors. First, since only visible imagery is used, wave clouds that form during nighttime hours but dissipate before daytime, will not be identified. The daytime limitation affects also our estimates of the wave event duration, in case of wave events that formed during daylight and extended into nighttime hours or wave events that formed during the night and extended into the daylight hours. Figure 3 shows this error as a function of month, revealing the largest errors for the months of January to April. While the infrared imagery would help to mitigate this problem by allowing detection of wave clouds during nighttime, the resolution of infrared imagery at 8 km that was available to us proved insufficient to discern fine-scale features characterizing the majority of detected wave clouds. The second limitation arising from the use of visible satellite imagery is that wave clouds can form underneath higher cloud layers of solid overcast. While very high amplitude waves may be able to penetrate these cloud layers, most wave clouds will be hidden from the satellite’s view. Finally, since the satellite imagery is only 1 km resolution, wave clouds must be relatively large to be identifiable. Small mountain wave clouds as well as rotor clouds, low-level cumuliform clouds

underneath mountain wave crests that frequently develop in the lee of the Sierra Nevada, are not large enough to be identified in the 1 km imagery. It should be noted that all of these limitations lead to *underrepresentation* of wave event numbers. Therefore, the climatology presented here represents lower limits of the frequency of mountain wave events.

### 3 Climatology Results

This satellite climatology was obtained for two recent seasons, 1999-2000 and 2000-2001. While two seasons is far too little to draw final conclusions, it is possible to make some preliminary conclusions on the distribution of mountain waves by type, month, and location.

#### 3.1 Wave Type Distribution

Table 1 shows the number of events that occurred each month in any region of the Sierra Nevada. In the seasonal totals, lee waves were more common than single wave events by a factor of over 1.5, constituting slightly over 60% of all wave events. However, the ratio of the two types of wave events was not consistent for each month. November and December contained nearly equal numbers of lee waves and single waves during each of the two seasons. January and May of 2000 also contained comparable numbers of lee waves and single waves. The remaining months, including January and May of 2001, were characterized by a clear dominance of lee wave events, often exceeding two times the number of single wave events. On several occasions only one or two single waves cloud events were reported for the entire month.

#### 3.2 Monthly Distribution

Excluding the extreme variations in January and May, the rest of the months exhibit a similar pattern between the two seasons (Figure 4). Each season begins with October as one of

the months with the fewest reported events. The number of events rise to a consistent relative maximum in November, followed by a near negligible decrease in December. Skipping the large fluctuations observed in January, February contains a similar number of events as November and December. This is followed by a decrease to a relative minimum in March and then a sharp increase to a large maximum in April, during which a wave event occurs somewhere in the Sierra Nevada on average two out of three days.

### **3.3 Spatial Distribution**

Table 2 shows the number of events which occurred in each region of the Sierra, including single events which occurred simultaneously in more than one region. The overall distribution of wave events between north and south varied significantly between the two seasons. In the 99–00 season, there was a nearly equal number of north and south wave events, whereas in the 00–01 season there were nearly two times more wave events in the north compared to the south. This difference is consistent with the inter-seasonal difference in the number of wave events in January and May, as nearly half of all wave events in the southern Sierra Nevada in the 99–00 season had occurred within these two months.

The region of formation most strongly affects the wave type. In both seasons, approximately 80% of all northern wave events were lee waves. In the southern region, the percentage of lee waves varied from 40% in one season to under 20% in the other, whereas the number of single wave events was fairly constant between the two seasons. From this, it appears that lee wave trains are more common in the northern Sierra and single waves appear to be more common in the southern Sierra Nevada.

In addition to waves that formed in a particular region, wave events that covered the entire length of the Sierra Nevada were also recorded. The large inter-seasonal difference is evident also

in the number of these events, which were twice as frequent in the 99–00 season compared to the subsequent one. Overall, these events made up between 15% and 30% of all the events in a given season. Over 75% of the events that extended over the entire length of the Sierra were lee wave trains.

### 3.4 Trapped Lee Wave Wavelength

Figure 5 shows wavelength histograms for the trapped lee wave events in the two wave seasons. The minimum detected wavelength was 4 km and the maximum 32 km. This wavelength span was divided into 7 equidistant bins, each 4 km wide. The total number of trapped lee wave events shown in the two seasons is similar, with 79 and 64 trapped lee wave events in the 99–00 and 00–01 seasons, respectively (cf. Table 1).

In both seasons, the largest percentage of lee wave events (35% in 99–00 and 45% in 00–01) falls in the wavelength range of 8–12 km. In both seasons, approximately 90–95% of trapped lee waves had the wavelength shorter than 20 km. The inter-seasonal variation is reflected in the wavelength diagrams as well, with about equal number (45%) of trapped waves with wavelength in the range of 4–12 km and 12–20 km in the 1999–2000 season, compared to a clear predominance of shorter wavelength trapped waves ( $\sim 70\%$  of all events) in the 2000–2001 season. This is also reflected in the average and median wavelengths, which are equal to 13.3 and 12.4 km in the 1999–2000 season and 10.7 and 9.6 km in 2000–2001.

### 3.5 Discussion

Figures 4 and 6 summarize the results on the monthly and spatial distribution of wave events discussed above. While these results are based on a limited data set and may not accurately represent long-term average conditions, some patterns are sufficiently pronounced so that it is

reasonable to speculate as to the physical processes that might lead to their existence.

Generally there appears to be a predominance of wave events in the northern Sierra Nevada over the southern Sierra (Fig. 6). As indicated earlier, the conditions necessary for mountain wave and wave cloud formation in the lee of the Sierra Nevada are typically found near frontal zones of mid-latitude cold fronts associated with an upper-level trough along the Pacific coast (Holmboe and Klieforth 1957). Strong westerly or southwesterly flow across the Sierra range favorable for wave generation is found at the base of this trough; however, the trough must extend sufficiently far southward for this to occur. It is clear that the typical low off the Pacific Northwest will extend its associated trough into the northern Sierra more often than into the southern Sierra, leading to a larger proportion of wave events in the lee of the northern Sierra as reflected in our statistics.

Large inter-annual variability in the number of events, such as observed for January and May (Fig. 4), can also be related to the synoptic-scale forcing. As Fig. 7 shows, differences in the number of wave events observed in January and May 2000 and 2001 is reflected well in the persistence of strong westerly winds at 700 hPa level in the 35–40° N latitude band in these two months in 2000 and their general absence in 2001. This is not surprising given that moderate to strong ridge-perpendicular wind ( $\geq 10 \text{ m s}^{-1}$ ) at ridge-level height is one of the necessary conditions for wave generation. Some of these long periods of strong cross-mountain winds are due to unusually persistent cutoff lows or blocking highs located off the southern California coast (Fig. 8). Thus, to a large degree the interannual variability of the number of wave events observed in January and May in these two successive wave seasons can be explained by the variability of the synoptic-scale forcing.

In terms of duration, single wave events appear in general to have shorter duration than lee wave events. There is some indication also of much longer wave event duration in April and May. Given that April is among months with the largest underestimate of event duration (cf. Fig. 3), it

is quite plausible that April is the month with the longest lasting wave events in the Sierra Nevada.

The lee wave train is clearly a more common wave form in the northern Sierra, whereas the single wave cloud is found to be a more common feature in the southern Sierra Nevada. In order to examine to what degree is this difference in the wave form conditioned by the upstream environment, we have examined the upstream profiles of wind and stability for trapped lee wave and single wave events in both the northern and southern Sierra Nevada. The Scorer parameter profiles,

$$l^2(z) = \frac{N^2(z)}{U^2(z)} - \frac{1}{U^2} \frac{\partial^2 U(z)}{\partial z^2}, \quad (1)$$

where  $N$  is the Brunt-Väisälä frequency and  $U$  is the component of the wind normal to the Sierra ridge, were computed from available Oakland soundings for the northern wave events and from available Vandenberg soundings for the southern events. The total number of northern events for which Oakland soundings were available at nearby times are 66 and 11 for trapped and single wave events, respectively. The corresponding numbers for the south are 19 trapped and 32 single wave events with available Vandenberg soundings. Virtual potential temperature and mountain normal wind speed (assuming a mean orientation of 6 degrees west of north) were calculated at each sounding level and interpolated to a 50 m grid for finite differencing. Sliding average filters were applied to the vertical profile of each variable to eliminate small-scale noise from the Scorer parameter curvature term, arising from the computation of the second derivative.

Based on theoretical arguments, the decrease with height of the Scorer parameter is expected for lee wave trapping, whereas vertical propagation of wave energy is favored by a relatively constant Scorer parameter profile. As expected, in more than half of all the lee wave cases, a sharp decrease of Scorer parameter with height was associated with stable layers due to temperature inversions within strongly vertically sheared flow. However, such stable layers were also present in about one third of single wave events. Thus, as a quantitative measure of the Scorer parameter layering,

we have computed a decrease of the Scorer parameter over a 2 km deep layer above the ridge height, expressed as a percentage of the Scorer parameter value at the bottom of this layer. For the average ridge height we specified 2.5 km for the northern Sierra and 3.5 km for the southern Sierra. The average values for the trapped and single wave events are shown in Table 3. Given the spread in altitude of significant Scorer parameter layering, the numbers in Table 3 represent likely an underestimate for the lee wave cases. Nevertheless, it is clear that the Scorer parameter drop in the lee wave cases is on average larger than that for the single wave cases. The difference becomes even more pronounced if from all single wave events one isolates only cases with no temperature inversion. Due to the smallness of the northern sample size, in Table 3 we show this last category for the southern Sierra only. These results are consistent with the expectation that the difference in wave propagation characteristics, described by Scorer parameter, has to exceed a certain threshold value before the wave trapping can occur (Durran 1990).

It is necessary to point out that operational soundings are not always available at the same time as the wave clouds in satellite imagery, and so it is possible that the soundings used are not capturing the representative conditions. However, given about one third of the single wave cases with strong inversions, it is also possible that some of the single wave clouds are not indicative of vertically propagating waves, but are actually associated with trapped lee waves whose amplitude decreases rapidly downstream, leaving only a single wave cloud in the lee (Grubišić and Billings 2007). The decrease of wave amplitude downwind can be due to an interference of a mountain range located in the lee, such as the White-Inyo range that can change the phase and/or amplitude of lee waves generated by the Sierra Nevada. In case of the positive interference or resonance, rotors that form underneath the first wave crest in the Sierra Nevada lee under those conditions can cause significant dissipation of wave energy and lead to decrease of lee wave amplitude downwind. Rather than differing upstream conditions for different type of wave clouds, the presence of the White-Inyo

mountain range and the formation of rotors may be contributing to some of the single mountain wave clouds in the southern portion of the Sierra Nevada. The investigation of reasons for such a wave behavior is beyond the scope of this study.

## 4 Conclusions

This note delivers a satellite-based climatology of the Sierra Nevada mountain wave events. GOES-10 visible satellite imagery was visually examined for the presence of wave clouds during two wave seasons in the period of 1999 to 2001, including months from October to May. Two type of wave clouds were defined, the lee wave trains and single wave clouds, and these were detected based on their location, shape and texture. As mountain waves can be present without wave clouds, the results presented here represent lower limits of the frequency of mountain wave events in the lee of the Sierra Nevada.

The frequency of occurrence of two wave types is shown as a function of the month of occurrence (October to May) and region of formation (north, middle, south, or the entire Sierra Nevada range). Results indicate that the maximum number of mountain wave events in the lee of the Sierra Nevada occurs in the month of April. For several months, including January and May, frequency of wave events displays substantial interannual variability that is shown to be closely related to the interannual variability of synoptic-scale flows. Overall, trapped lee waves appear to be more common, in particular in the lee of the northern Sierra Nevada. The average wavelength of the Sierra Nevada lee waves was found to lie between 10 and 15 km, with a minimum at 4 km and a maximum at 32 km. A single wave cloud on the lee side of the mountain range was found to be a more common feature in the southern Sierra Nevada. While single wave clouds are expected to be signatures of the vertically propagating waves, it is hypothesized that a certain fraction of these events are trapped lee waves whose amplitude decreases rapidly downwind due to the presence of

a parallel downwind range in the southern Sierra, the White-Inyo mountains.

*Acknowledgments.*

This study was initiated as an undergraduate summer research project for Stephanie Cardon, while she was a recipient of the Nevada EPSCoR Young Scholars Fellowship. We are indebted to Stephanie for her diligent work that provided the basis for the current study. The source of the GOES-10 imagery was the Naval Research Laboratory (NRL) in Monterey, CA, and we thank the NRL staff for making this data available to us. Constructive comments and ideas received in the course of this work from Larry Armi, Jim Doyle, Joachim Kuettner, and Rich Rotunno are much appreciated. The Hovmoller images are provided by the NOAA-CIRES/Climate Diagnostics Center, Boulder Colorado and obtained from their Web site at <http://www.cdc.noaa.gov/>. This research has been supported in part by the National Aeronautical and Space Administration EPSCoR Program, Grant NCC5-397 (subaward UCCSN-99-899), and the National Science Foundation, Division of Atmospheric Science, Grants ATM-0002735 and ATM-0242886.

## References

- Auer, A. A., 1992: Wave cloud formations in the lee of southern New Zealand. *Weather*, **47**, 103–105.
- Banta, R. M., and C. B. Schaaf, 1987: Thunderstorm genesis zones in the Colorado Rocky Mountains as determined by traceback of geosynchronous satellite images. *Mon. Wea. Rev.*, **115**, 463–476.
- Brown, W. O. J., S. A. Cohn, V. Grubišić, and B. J. Billings, 2005: The Sierra Rotors Project, Observations of mountain waves. *13th Symposium on Meteorological Observations and Instrumentation*, Amer. Meteor. Soc., <http://ams.confex.com/ams/pdfpapers/94042.pdf>
- Chopra, K. P., and L. F. Hubert, 1965: Mesoscale eddies in wake of islands. *J. Atmos. Sci.*, **22**, 652–657.
- Clark, T. L., W. D. Hall, R. M. Kerr, D. Middleton, L. Radke, F. M. Ralph, P. J. Neiman, D. Levinson, 2000: Origins of aircraft-damaging clear-air turbulence during the 9 December 1992 Colorado downslope windstorm: Numerical simulations and comparison with observations. *J. Atmos. Sci.*, **57**, 1105–1131.
- Conover, J. H., 1964: The identification and significance of orographically induced clouds observed by TIROS satellites. *J. Appl. Meteor.*, **3**, 226–234.
- Durran, D. R., 1990: Mountain waves and downslope winds. In *Atmospheric Processes over Complex Terrain*, Ed. W. Blumen, Amer. Meteor. Soc, 323 pp.
- Fritz, S., 1965: The significance of mountain lee waves as seen from satellite pictures. *J. Appl. Meteor.*, **4**, 31–37.

- Grubišić, V., and B. J. Billings, 2007: The intense lee-wave rotor event of Sierra Rotors IOP 8. *J. Atmos. Sci.*, In press.
- Grubišić, V., J. D. Doyle, J. Kuettner, G. S. Poulos, and C. D. Whiteman, 2004: Terrain-induced Rotor Experiment (T-REX) Overview Document and Experiment Design. 72 pp. [http://www.eol.ucar.edu/projects/trex/documents/TREX\\_SOD.pdf](http://www.eol.ucar.edu/projects/trex/documents/TREX_SOD.pdf)
- Holmboe, J., and H. Klieforth, 1957: Investigation of mountain lee waves and the air flow over the Sierra Nevada. Final Report. Department of Meteorology, UCLA, Contract AF 19(604)–728, pp. 283.
- Hubert, L. F., and A. F. Kureger, 1962: Satellite pictures of mesoscale eddies. *Mon. Wea. Rev.*, **90**, 457–463.
- Jiang, Q., and J. D. Doyle, 2006: Topographically generated cloud plumes. *Mon. Wea. Rev.*, **134**, 2108–2127.
- Johnson, D. B., P. Flament, and R. L. Bernstein, 1994: High-resolution satellite imagery for mesoscale meteorological studies. *Bull. Amer. Meteor. Soc.*, **75**, 5–234.
- Kuettner, J. P., 1959: The rotor flow in the lee of mountains. GRD Research Notes, No. 6, AFCRC–TN–58–626. ASTIA Document No. AD–208862, pp. 20.
- Lilly, D., and E. J. Zipser, 1972: The Front Range windstorm of 11 January 1972—A meteorological narrative. *Weatherwise*, **25(2)**, 56–63.
- Mitchell, R. M., Cechet, R. P., Turner, P. J., and C. C. Elsum, 1990: Observation and interpretation of wave clouds over Macquarie Island. *Quart. J. Roy. Meteor. Soc.*, **116**, 741–752.
- Moore, G. W. K., and I. A. Renfrew, 2005: Tip jets and barrier winds: A QuikSCAT climatology of high wind speed events around Greenland. *J. Climate*, **18**, 3713–3725.

- Pan, F., and R. B. Smith, 1999: Gap winds and wakes: SAR observations and numerical simulations. *J. Atmos. Sci.*, **56**, 905–923.
- Peak, J. E., and P. M. Tag, 1992: Toward automated interpretation of satellite imagery for Navy shipboard applications. *Bull. Amer. Meteor. Soc.*, **73**, 995–1008.
- Ralph, F. M., M. Crochet, and S. V. Venkateswaran, 1992: A study of mountain lee waves using clear-air radar. *Quart. J. Roy. Meteor. Soc.*, **118**, 597–627.
- Ralph, F. M., P. J. Neiman, T. L. Keller, D. Levison, and L. Fedor, 1997: Observations, simulations, and analysis of nonstationary trapped lee waves. *J. Atmos. Sci.*, **54**, 1308–1333.
- Scorer, R. S., 1986: *Cloud Investigation by Satellite*. Ellis Horwood. Halsted Press. 300 pp.
- Smith, R. B., 1976: The generation of lee waves by the Blue Ridge. *J. Atmos. Sci.*, **33**, 507–519.
- Smith, R. B., 1979: The influence of mountains on the atmosphere. *Advances in Geophysics*, Vol. 21, Academic Press, 87–230.
- Smith, R. B. and V. Grubišić, 1993: Aerial observations of Hawaii’s wake. *J. Atmos. Sci.*, **50**, 3728–3750.
- Smith, R. B., A. Gleason, P. Gluhosky, and V. Grubišić, 1997: The wake of St. Vincent. *J. Atmos. Sci.*, **54**, 606–623.
- Vosper, S. B., and S. D. Mobbs, 1996: Lee waves over the English Lake district, *Quart. J. Roy. Meteor. Soc.*, **122**, 1283–1305.
- Vosper, S. B., and R. M. Worthington, 2002: VHF radar measurements and model simulations of mountain waves over Wales. *Quart. J. Roy. Meteor. Soc.*, **128**, 185–204.

Whelan, R. F., 2000: *Exploring the Monster. Mountain Lee Waves: The Aerial Elevator*. Wind Canyon Books Inc., 169 pp.

Worthington, R. M., and L. Thomas, 1996: Radar measurements of critical-layer absorption in mountain waves. *Quart. J. Roy. Meteor. Soc.*, **122**, 1263–1282.

Table 1: Wave Type Distribution and Total Number of Wave Events by Month

	October	November	December	January	February	March	April	May	Total
1999-2000									
Lee Waves	3	9	7	15	14	6	14	11	79
Single Waves	1	8	6	11	2	2	9	10	49
All Waves	4	17	13	26	16	8	23	24	128
2000-2001									
Lee Waves	9	8	6	5	10	11	12	3	64
Single Waves	4	7	9	2	5	1	7	1	36
All Waves	13	15	15	7	15	12	19	4	100

Table 2: Distribution of Wave Events by Region

	North	Central	South	Entire Length
1999-2000				
Lee Waves	32	20	19	29
Single Waves	9	16	28	7
All Waves	41	36	47	36
2000-2001				
Lee Waves	42	25	5	12
Single Waves	10	7	21	4
All Waves	52	32	26	16

Table 3: Percentage Decrease of Scorer Parameter

	Lee	Single	Single NI
North	69.4	62.4	
South	67.9	61.1	56.9

## List of Figures

1	Topography of the Sierra Nevada. Bold dashed lines represent borders between different regions of the Sierra range defined in this study. . . . .	24
2	GOES-10 visible images of (a) a single wave cloud in the northern Sierra Nevada, (b) trapped lee waves in the northern Sierra Nevada, (c) a single wave cloud in the southern Sierra Nevada, and (d) trapped lee waves in the northern Sierra Nevada and a single wave cloud in the southern Sierra Nevada with a cirrus cloud deck. . .	25
3	Box diagram of the onset times (lower boxes) and end times (upper boxes) of all detected wave events as a function of month. The boxes indicate the spread of data between the first and third quartile. The horizontal lines within boxes mark medians, and bars indicate the extrema. Solid yellow and blue lines show times of sunrise and sunset. . . . .	26
4	Total number of wave events anywhere in the lee of the Sierra Nevada by month for the 1999-2000 and 2000-2001 seasons. . . . .	27
5	Histograms of the horizontal wavelength of trapped lee waves for the 1999-2000 and 2000-2001 seasons. The total number of events for the two seasons is 79 and 64, respectively. . . . .	28
6	Average number of observed wave events for (a) northern Sierra Nevada and (b) southern Sierra Nevada. The three columns for each month show the number of lee wave trains, single wave clouds, and the total for that month. Event duration is indicated by hatching; more than 7.5 hours (solid), between 5 and 7.5 hours (diagonal hatched), and less than 5 hours (vertically hatched). . . . .	29

7	<p>Time-longitude diagrams of the mean daily westerly wind component at 700 hPa for latitudes 35–40° for (a) January 2000, (b) January 2001, (c) May 2000, and (d) May 2001. The data shown is from the NCAR/NCEP reanalysis. The longitude span of the Sierra range (~118–122° W) is marked with thick solid lines. Stars on the y-axis marks days with detected wave events along the Sierra Nevada lee. . . . .</p>	30
8	<p>700 hPa analysis for 12 UTC 15 May 2000 during a persistent 5-day period of mountain wave activity. (From National Climatic Data Center.) . . . . .</p>	31

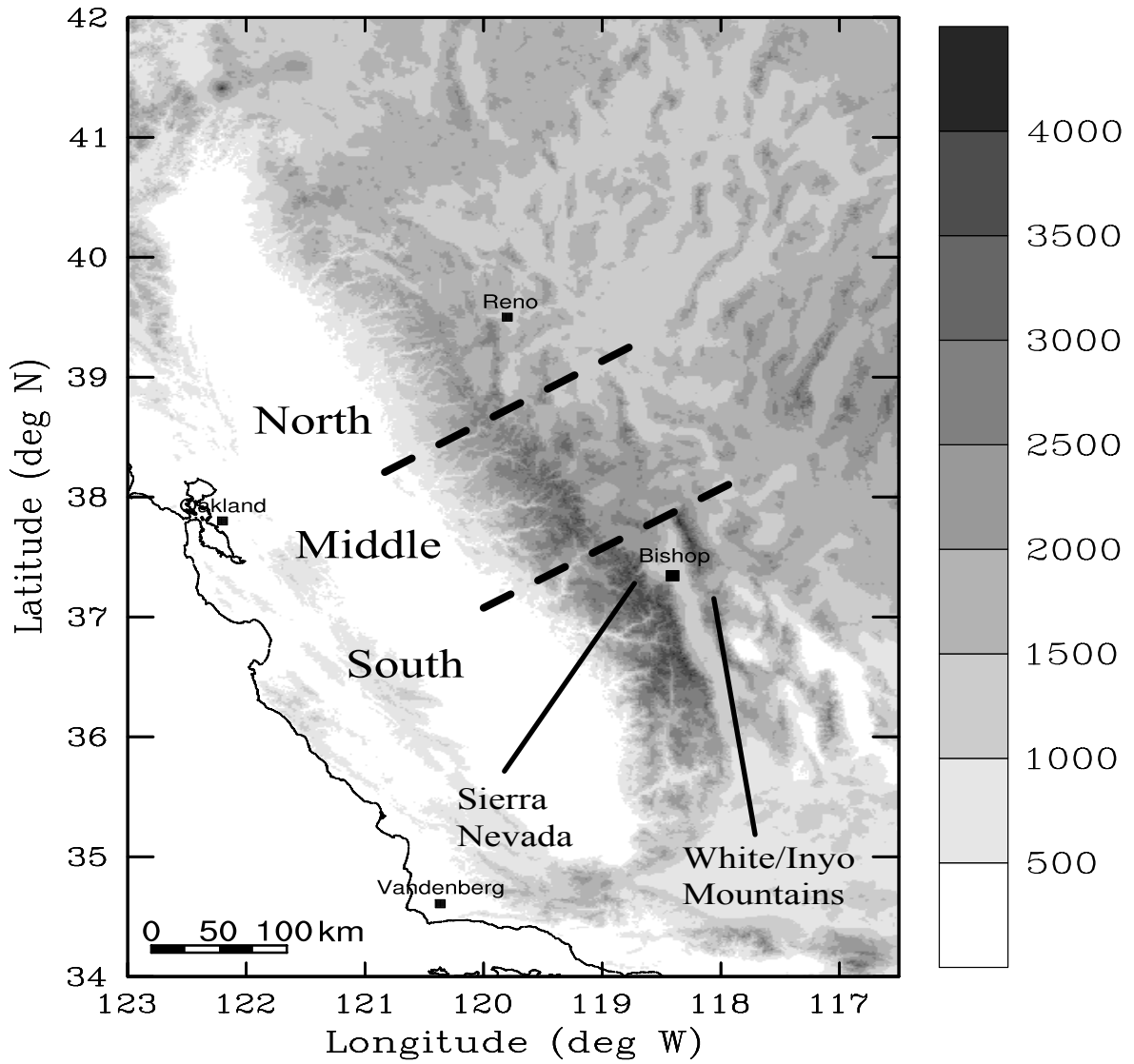


Figure 1: Topography of the Sierra Nevada. Bold dashed lines represent borders between different regions of the Sierra range defined in this study.

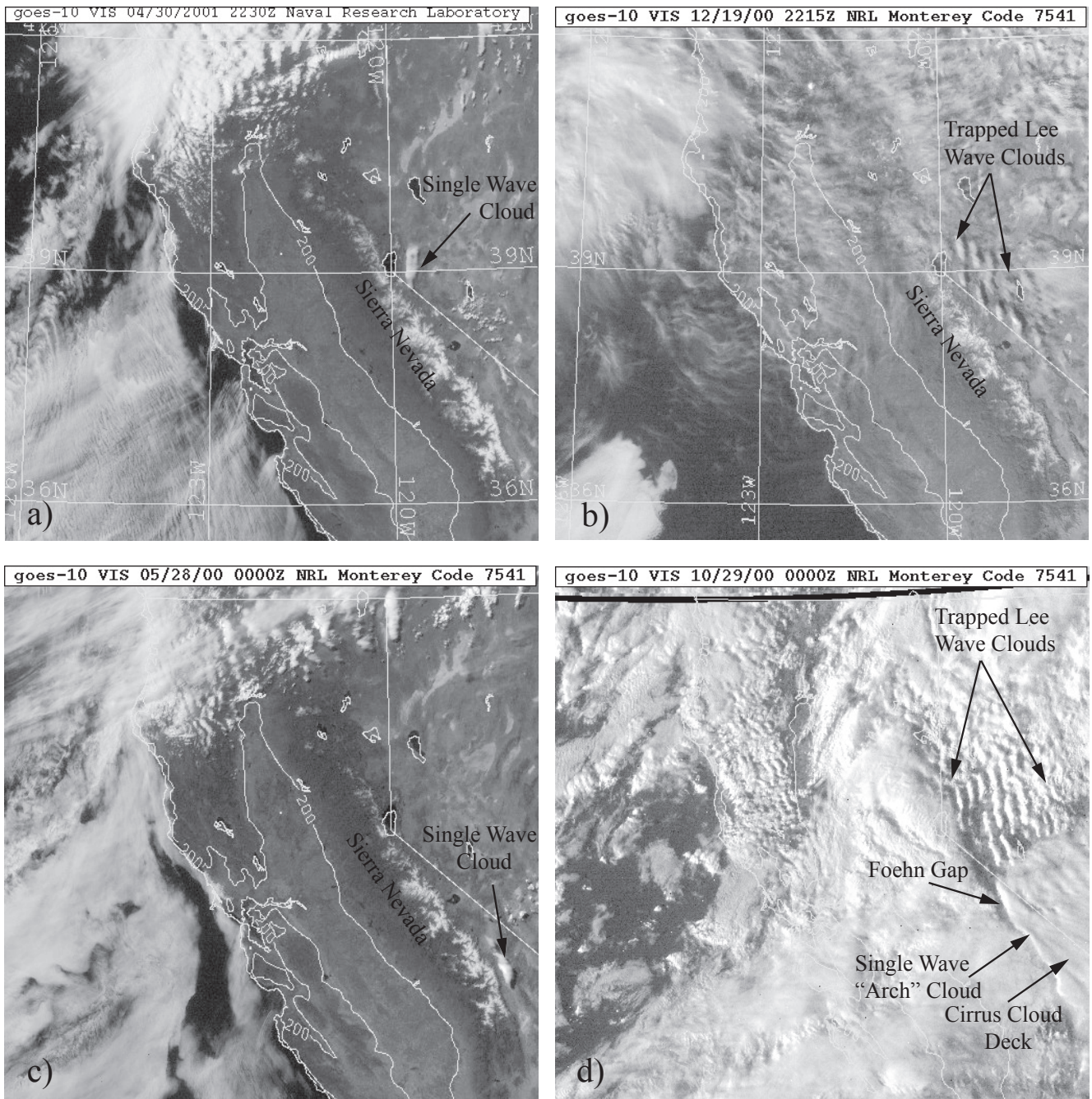


Figure 2: GOES-10 visible images of (a) a single wave cloud in the northern Sierra Nevada, (b) trapped lee waves in the northern Sierra Nevada, (c) a single wave cloud in the southern Sierra Nevada, and (d) trapped lee waves in the northern Sierra Nevada and a single wave cloud in the southern Sierra Nevada with a cirrus cloud deck.

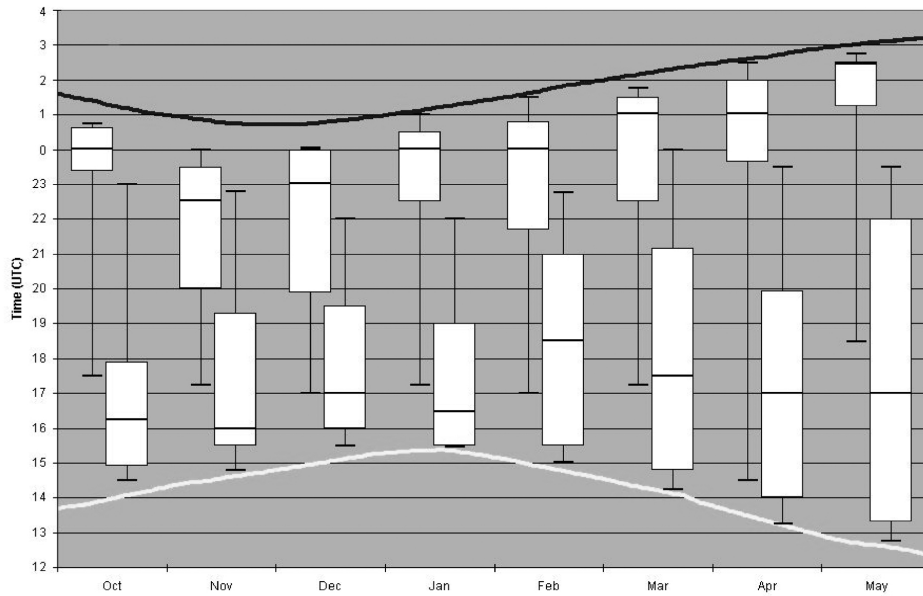


Figure 3: Box diagram of the onset times (lower boxes) and end times (upper boxes) of all detected wave events as a function of month. The boxes indicate the spread of data between the first and third quartile. The horizontal lines within boxes mark medians, and bars indicate the extrema. Solid yellow and blue lines show times of sunrise and sunset.

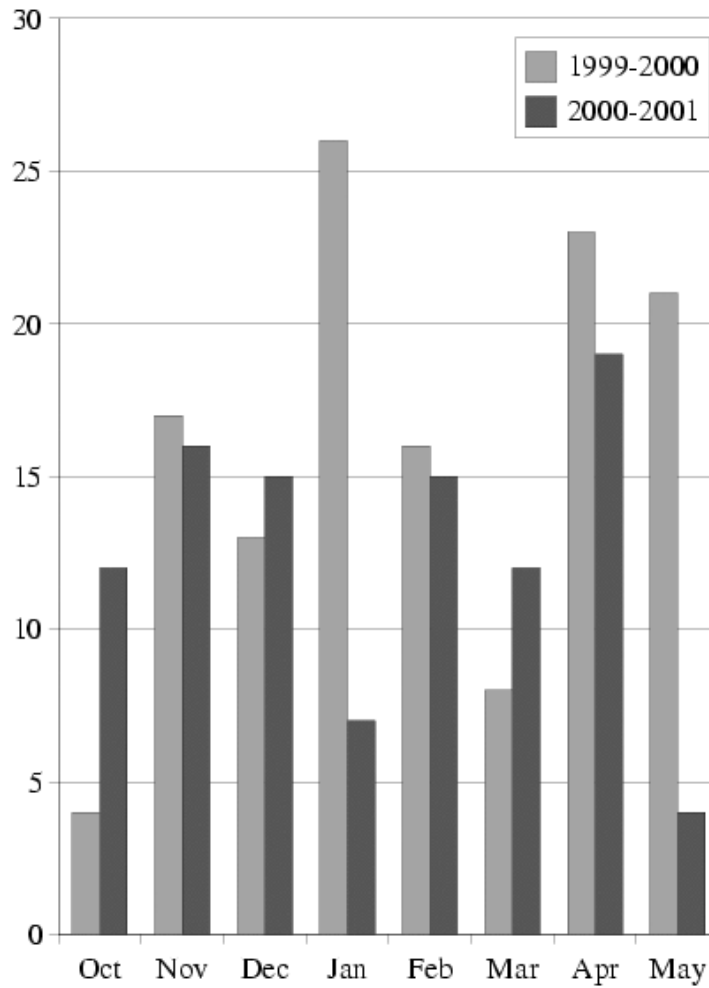


Figure 4: Total number of wave events anywhere in the lee of the Sierra Nevada by month for the 1999-2000 and 2000-2001 seasons.

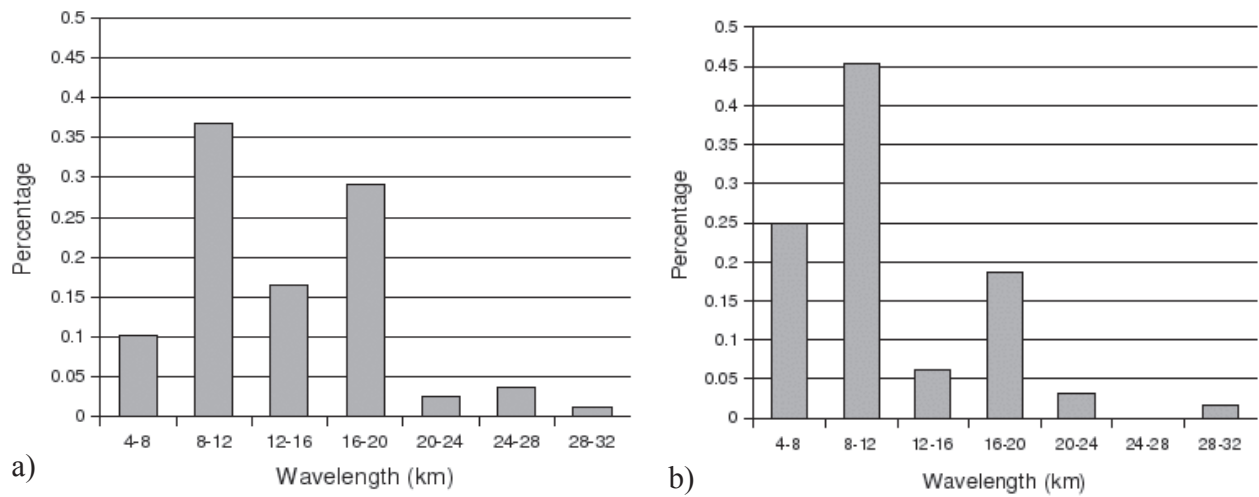


Figure 5: Histograms of the horizontal wavelength of trapped lee waves for the 1999-2000 and 2000-2001 seasons. The total number of events for the two seasons is 79 and 64, respectively.

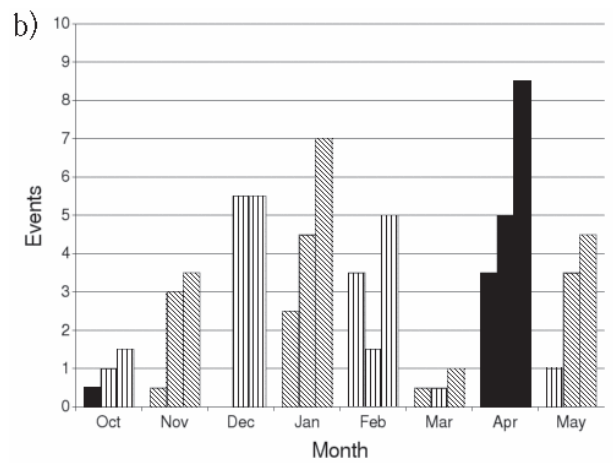
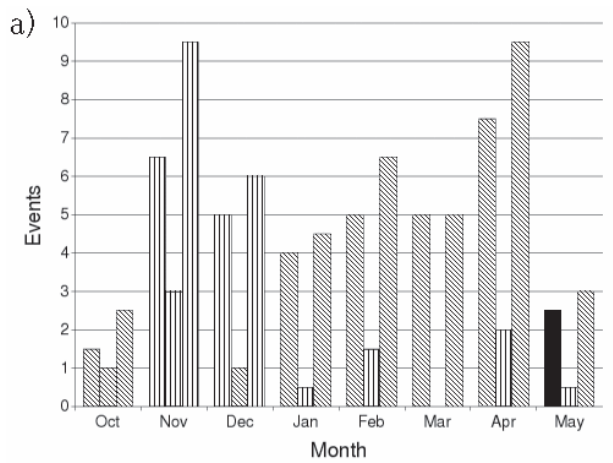


Figure 6: Average number of observed wave events for (a) northern Sierra Nevada and (b) southern Sierra Nevada. The three columns for each month show the number of lee wave trains, single wave clouds, and the total for that month. Event duration is indicated by hatching; more than 7.5 hours (solid), between 5 and 7.5 hours (diagonal hatched), and less than 5 hours (vertically hatched).

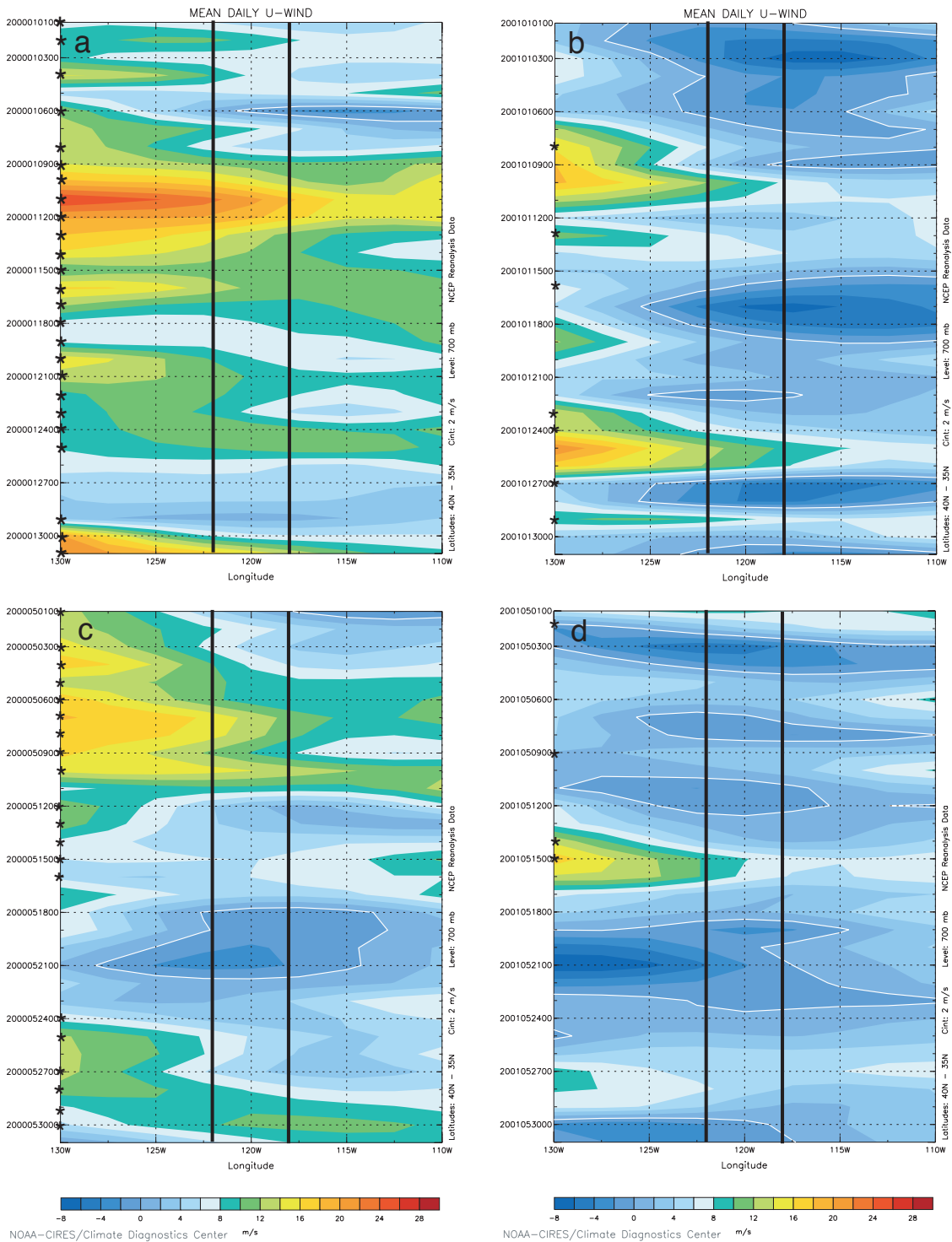


Figure 7: Time-longitude diagrams of the mean daily westerly wind component at 700 hPa for latitudes 35–40° for (a) January 2000, (b) January 2001, (c) May 2000, and (d) May 2001. The data shown is from the NCAR/NCEP reanalysis. The longitude span of the Sierra range (~118–122° W) is marked with thick solid lines. Stars on the y-axis marks days with detected wave events along the Sierra Nevada lee.

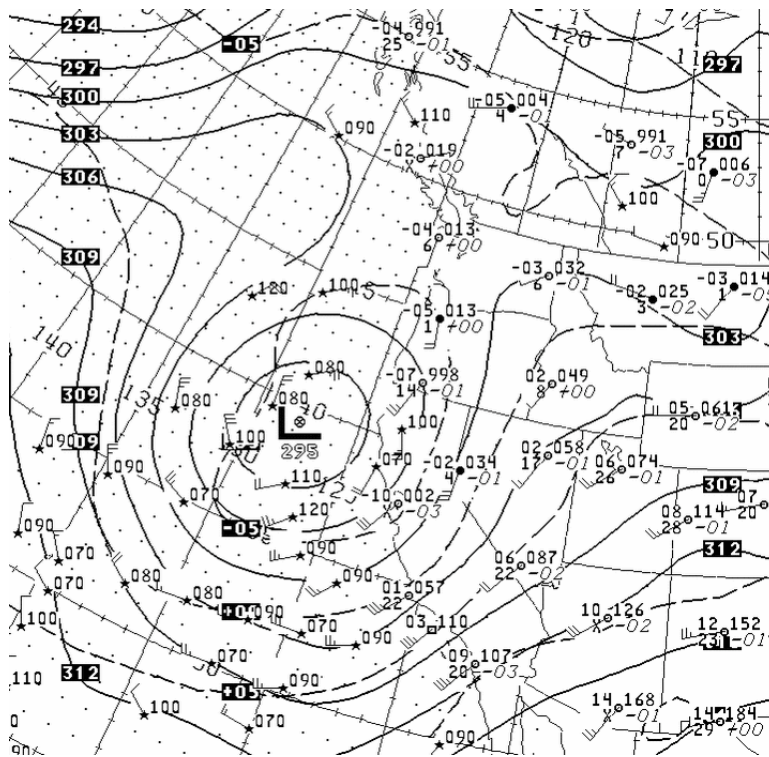


Figure 8: 700 hPa analysis for 12 UTC 15 May 2000 during a persistent 5-day period of mountain wave activity. (From National Climatic Data Center.)